Acyl Structure Regulates Galactosylceramide's Interfacial Interactions†

Shaukat Ali,‡ Janice M. Smaby, and Rhoderick E. Brown*

The Hormel Institute, University of Minnesota, Austin, Minnesota 55912

Received May 14, 1993; Revised Manuscript Received August 26, 1993®

ABSTRACT: Galactosylceramides (GalCer) with homogeneous acyl chains containing zero, one, or two *cis* double bonds have been synthesized and characterized at an argon–aqueous buffer interface using a Langmuir film balance. Both surface pressure and surface potential were measured as a function of molecular area at 24°C. *N*-Lignoceroylgalactosylsphingosine (*N*-24:0-GalSph), *N*-stearoylgalactosylsphingosine (*N*-18:0-GalSph), and *N*-palmitoylgalactosylsphingosine (*N*-16:0-GalSph) form condensed films that are similar to that of bovine brain GalCer, which contains long saturated and mono-unsaturated acyl chains, almost half being hydroxylated. In contrast, a bovine brain GalCer subfraction (NFA-GalCer) that is devoid of the hydroxylated acyl chains displays an apparent two-dimensional phase transition near 9.0 mN/m at 54 Å^2/molecule. To determine the role of acyl unsaturation in regulating NFA-GalCer's surface behavior, GalCer derivatives containing different mono-unsaturated acyl residues were investigated. *N*-Nervonoylgalactosylsphingosine (*N*-24:1$^{\Delta 15}$-GalSph) and *N*-docosenoylgalactosylsphingosine (*N*-22:1$^{\Delta 13}$-GalSph) show liquid-expanded to -condensed phase transitions in their force–area isotherms at 10 and 35 mN/m, respectively. Introduction of acyl chains that are short and saturated [e.g., *N*-decanoylgalactosylsphingosine (*N*-10:0-GalSph)] or that are long but contain two *cis* double bonds [e.g., *N*-linoleoylgalactosylsphingosine (*N*-18:2$^{\Delta 9,12}$-GalSph)] causes GalCer to display only liquid-expanded behavior at 24°C. The surface potentials (ΔV) of the condensed GalCer derivatives with long saturated acyl residues were quite similar and were over 100 mV higher than that of bovine brain GalCer. In contrast, ΔV values for GalCer derivatives containing mono-unsaturated acyl chains and displaying liquid-expanded behavior were 60 mV lower than that of bovine brain GalCer. Upon onset of the liquid-expanded to -condensed phase transition, the slope of the ΔV–A isotherms increased. Interestingly, in the condensed phase, *N*-24:1$^{\Delta 15}$-GalSph reached significantly higher levels of ΔV, resulting in a surface dipole moment approximately 4 times higher than that of bovine brain GalCer.

Certain glycosphingolipids and their metabolites appear to play important roles in promoting regeneration of nerve cells, in regulating protein kinase C activity, and in modulating hormone receptor function (Ledeen, 1984; Hannun & Bell, 1989; Hakomori, 1990). In addition, several pathogenic bacteria, viruses, and bacterial toxins are known to bind specifically to glycosphingolipids during invasion of cells (Karlsson, 1989). The glycosphingolipids need not be multiglycosylated or sialylated to act in such a capacity. For instance, monoglycosylated ceramides such as galactosylceramide (GalCer)[1] can serve as cell surface receptors for the gp120 glycoprotein of type 1 human immunodeficiency virus (Harouse et al., 1991; Bhat et al., 1991). Thus, it is important to understand the structural features of GalCer responsible for its distribution and accessibility within membranes.

Studies carried out on naturally occurring GalCer reveal unusual physical properties (Thompson & Tillack, 1985; Curatolo, 1987). For instance, aqueous dispersions of GalCer isolated from bovine brain have the capacity to form extraordinarily stable lamellar crystalline phases near physiological temperature (Bunow, 1979; Curatolo, 1982; Curatolo & Jungawala, 1985; Lee et al., 1986). Moreover, Fourier transform infrared spectroscopic studies suggest that multiple lateral domains enriched in various GalCer molecular species may co-exist in aqueous dispersions of bovine brain GalCer (Jackson et al., 1988). Although it is tempting to attribute bovine brain GalCer's unusual properties to the abundance of long, saturated fatty acyl residues, such conclusions are not necessarily valid. For instance, increasing the acyl chain length in GalCer from palmitate to stearate or to lignocerate produces little change in the high-enthalpy, lamellar crystal to liquid crystal phase transition temperature (Ruocco et al., 1981; Curatolo & Jungalwala, 1985; Reed & Shipley, 1987; 1989) and has little effect on mixing behavior with dipalmitoyl phosphatidylcholine (DPPC) (Ruocco et al., 1983; Gardam & Silvius, 1989). These unusual properties have often been attributed to GalCer's ability to form intermolecular hydrogen bonds [e.g., Bunow and Levin (1980) and Pink et al. (1988)]. Whatever the reason, overcoming GalCer's unique intermolecular interactions requires other changes in acyl chain structure. For instance, we and others have examined the effect of acyl chain unsaturation on GalCer's phase properties. Introducing *cis* unsaturation into GalCer's acyl chains dramatically lowers its high-enthalpy crystal to liquid crystal transition temperature (Reed & Shipley, 1989) and strongly influences interfacial mixing behavior with phosphatidylcholines (Ali et al., 1991). What is not clear is the effect of acyl chain saturation and unsaturation on GalCer's interfacial interactions with other lipids.

† This research, which was supported by United States Public Health Service Grant GM45928 and the Hormel Foundation, also benefited from a NMR instrumentation grant (RR04654) provided through the Division of Research Resources of the National Institutes of Health.

* Address correspondence to this author.

‡ Present address: Division of Digestive Diseases, Room F231, New York Hospital–Cornell Medical Ctr., 525 East 68th St., New York, NY 10021 [FAX (212)746–8447].

® Abstract published in *Advance ACS Abstracts,* October 15, 1993.

[1] Abbreviations: GalCer, galactosylceramide; π, surface pressure; ΔV, surface potential; GalSph, galactosylsphingosine; LE, liquid-expanded; LC, liquid-condensed; MGDG, monogalactosyl diglyceride; GalSpd, deacylated GalCer with heterogeneous sphingolipid bases, usually sphingosine and dihydrosphingosine.

0006-2960/93/0432-11696$04.00/0

To provide a foundation for such studies, we first report the surface behavior of several homogeneously *N*-acylated GalCer species as determined using a Langmuir film balance. Using the monolayer technique permits individual lipid species to be studied over a range of molecular areas known to occur in membrane systems while it readily detects subtle alterations in intermolecular interactions and avoids changes in a mesophasic structure. The results provide a systematic characterization of the two-dimensional phase properties of different saturated and mono-unsaturated GalCer species, thus providing a framework for understanding interfacial interactions of GalCer molecules with each other as well as with other membrane lipids and proteins. This study helps provide insight into the membrane structural changes caused by accumulation of galactosylceramides in diseases such as globoid cell leukodystrophy (Suzuki & Suzuki, 1989) as well as by alteration of sphingolipid acyl composition which occurs in demyelinating diseases like adrenoleukodystrophy (Kishimoto et al., 1985). Preliminary reports including portions of this work have been presented elsewhere (Ali et al., 1992a,b).

MATERIALS AND METHODS

Lipid Synthesis. Bovine brain GalCer (Avanti Polar Lipids, Alabaster, AL) was deacylated by alkaline hydrolysis (Radin, 1974) and purified by medium-pressure flash chromatography on silicic acid (230–400 mesh) (Ali et al., 1991). The resulting psychosine (galactosylsphingoid, GalSpd) was fractionated according to sphingoid base composition (dihydrosphingosine versus sphingosine) by preparative TLC (1 mm thick silica gel GF plates; Analtech) using $CHCl_3/CH_3OH/NH_4OH$ (6:3:0.5). Then, the galactosylsphingosine (GalSph) was *N*-acylated with the desired homogeneous fatty acid using PPh_3/aldrithiol as reported previously (Ali et al., 1991). Products were fractionated by flash column chromatography using step gradients of $CHCl_3$ and $CHCl_3$/MeOH (98:2 and 90:10). Final purification of the desired *N*-acylated GalSph was accomplished by preparative TLC [$CHCl_3$/MeOH (85:15)]. Silicic acid coeluting with the GalCer was removed by passage through a C18 reverse-phase preparative column under medium pressure (Kubo & Hoshi, 1985). GalCer species were characterized by ^1H NMR (300 MHz): δ (ppm) 5.68–5.59 [1 H, dd, J = 7.4 and 15.0 Hz, C*H*(OH)=CH], 5.41–5.34 (1 H, dd, J = 7.4 and 15.2 Hz, CH=C*H*R), 4.15 (1 H, d, J = 6.71 Hz, galactosyl H1′), 3.82 (1 H, d, J = 2.75 Hz, galactosyl H4′), 3.78–3.72 (1 H, dd, J = 6.71 and 11.59 Hz, H6′^{a}–H5′, H6′^{a}–H6′^{b}), 3.69–3.64 (1 H, dd, J = 4.89 and 11.6 Hz, galactosyl H6′^{b}–H5′, H6′^{b}–Hd6′^{a}), 2.15–2.10 (2 H, t, J = 8.01 Hz, CH_2CO), 0.85 (6 H, t, J = 6.7 Hz, ω–CH_3s). Sphingosine content in the GalCer species (>98%) was analyzed by the method of Alvarez et al. (1989), and acyl chain homogeneity (>99%) was confirmed by GC-MS (Johnson & Brown, 1992). A GalCer stock solution was made in $CHCl_3$/MeOH/petroleum ether (5:1:4) and stored under nitrogen at −70°C. No degradation was seen when checked either by TLC or by surface pressure versus area behavior on the surface balance. The lipid concentration was determined by dry weight and by assaying nitrogen, as described elsewhere (Ali et al., 1991).

Solvents. Chloroform and methanol were distilled twice. Petroleum ether was distilled according to a procedure described elsewhere (Smaby & Brockman, 1985). Water was purified by reverse osmosis, mixed-bed deionization, adsorption charcoal, and filtration through a 0.2-μm polycarbonate membrane. The 10 mM potassium phosphate (pH 6.6) containing 100 mM NaCl and 0.02% NaN_3 was prepared fresh, filtered through a Diaflo hollow fiber sieve with a molecular mass cutoff of 10 000 Da (Amicon Corp., Danvers, MA), and stored under argon. Solvent purity was assessed as described by Ali et al. (1991) and by monitoring the surface potential versus molecular area behavior as described by Smaby and Brockman (1991a).

Monolayer Studies. A computer-controlled Langmuir-type film balance, calibrated with lipid standards according to their equilibrium spreading pressures (Smaby & Brockman, 1990) and housed in a laboratory equipped with a filtered air supply, was used to measure π–A and ΔV–A isotherms (Brockman et al., 1980). Glassware was acid cleaned and rinsed thoroughly with $CHCl_3$/MeOH (1:1). The solution of each lipid was spread in 51.7-μL aliquots onto a trough filled with ~800 ml of phosphate–saline buffer (pH 6.6). After a period of 4 min, to ensure the complete evaporation of solvents, the monolayer films were compressed at a rate of < 4 Å^2/molecule/min. Control experiments indicated that, with the exception of *N*-24:1$^{\Delta 15}$-GalSph, the π–A behavior of most GalCer species was reversible and reproducible upon consecutive compression–expansion–compression cycles at surface pressures below collapse. Further study will be required to address the details concerning the possible metastability in *N*-24:1-GalSph's behavior. The trough temperature was maintained at 24 ± 1°C through a temperature-controlled water bath. Surface potential was measured as a function of molecular area using a ^{210}Po ionizing electrode.

Analysis of Isotherms. Monolayer phase transitions between liquid-expanded and -condensed or between monolayer and bulk phases were identified using a combination of second and third derivatives of π with respect to A as previously described (Brockman et al., 1980, 1984).

π–A data of single-component lipid monolayers were analyzed by using a surface solution equation of state and by determining their compressibility. The equation of state (Smaby & Brockman, 1990, 1991b) is

$$\pi = (qKT/\omega_1) \ln\{(1/f_1)[1 + \omega_1/(A_\pi - \omega_0)]\} \quad (1)$$

where K is Boltzmann's constant, ω_1 is the cross-sectional area of an interfacial water molecule (9.65 Å^2), and ω_0 is the cross-sectional area of the dehydrated lipid, f_1 is the activity coefficient of interfacial water, and A_π is the total surface area divided by the number of lipid molecules present at each π. The scaling parameter q is correlated to f_1 (Smaby & Brockman, 1991b) and thus is not unique but does provide for an accurate description of the data because it allows for higher order terms involving the activity coefficient. Because data obtained near the high- and low-pressure limits can be especially sensitive to trace impurities [e.g., see Middleton and Pethica (1981)] and the dynamics of the experiment, the upper limit for reliable π–A data was determined as the value at which $d^2\pi/dA^2$ goes from positive to negative (typically 10–15% below π_t) and the lower limit was determined by the molecular area where π = 1.0 mN/m (Smaby & Brockman, 1990, 1991b). Over the range of π noted above, the ΔV–A behavior of the single component films can be described by

$$\Delta V = 37.7\mu_\perp/A + \Delta_{V0} \quad (2)$$

where ΔV is the potential measured in millivolts, and $\mu_\perp$ is the dipole moment (in millidebyes) perpendicular to the lipid–water interface (Smaby & Brockman, 1990) and is related to the slope of the ΔV versus $1/A$ plot. The intercept term, ΔV_0, is lipid-specific and appears to arise from an epitaxial ordering of interfacial water molecules during the transition

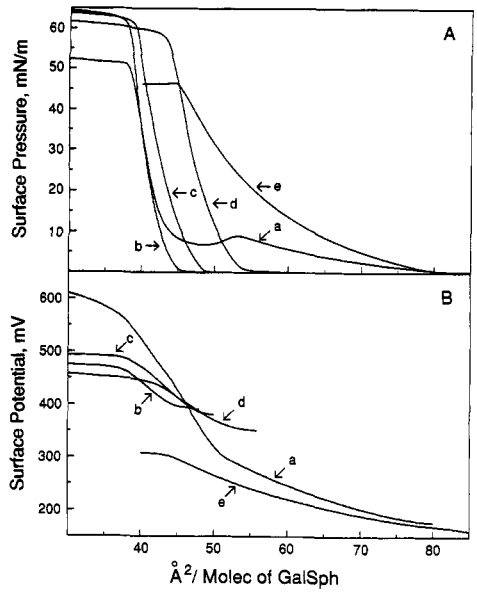

FIGURE 1: (A) Surface pressure vs molecular area (π–A) and (B) surface potential vs molecular area (ΔV–A) isotherms. Data were collected at 24°C as described under Materials and Methods for (a) NFA-GalCer, (b) N-24:0-GalSph, (c) N-18:0-GalSph, (d) N-16:0-GalSph, and (e) N-10:0-GalSph.

from the gaseous to the liquid-expanded state (Smaby & Brockman, 1990; Yokoyama & Kezdy, 1991).

Monomolecular film compressibility was calculated from π–A data using

$$k = (-1/A)(dA/d\pi) \quad (3)$$

where A is the area per molecule (Å^2) at the indicated surface pressures and π is the corresponding surface pressure in millinewtons per meter.

RESULTS

Surface Pressure vs Molecular Area of GalCer Species. To determine the role which acyl chain structure plays in regulating GalCer's intermolecular interactions, we synthesized several GalCer species that were greater than 99% homogeneous with respect to N-acyl chain composition and 98% homogeneous with respect to sphingoid base composition (see Materials and Methods). The resulting GalCer species contain 4-sphingenine (sphingosine), the predominant naturally occurring sphingoid base found in bovine brain GalCer. Prior to evaluation of the mixing behavior of these GalCer derivatives with cholesterol, π–A isotherms were determined for each GalCer derivative at an argon–buffered saline interface (24 °C). Because the present studies were aimed at determining the effects of increasing acyl hydrocarbon chain length and unsaturation on GalCer's behavior in surface films, we focused on GalCer derivatives containing nonhydroxylated fatty acyl residues. We compared their behavior with that of bovine brain GalCer that is also devoid of hydroxylated fatty acyl chains (NFA). Although π–A isotherms of NFA-GalCer have been published previously (Oldani et al., 1975; Johnston & Chapman, 1988), the conflicting results necessitated a careful reexamination of this natural compound's monolayer behavior. Our results are shown in Figure 1A (curve a).

NFA-GalCer forms monomolecular films that display complex, metastable force–area behavior at 24 °C. Liquid-expanded behavior occurs in NFA-GalCer films at surface pressures between 1 and 9 mN/m and at areas between 80 and 54 Å^2/molecule. Reduction of film area below 54 Å^2/molecule induces an apparent two-dimensional phase transition. The metastability of this transition is evident by the decline in surface pressure (1.5–2.0 mN/m) that precedes the rapid rise in film pressure between 48 and 40 Å^2/molecule. Apparent collapse occurs near 50 mN/m, and continuing compression to 25 Å^2/molecule reveals only a slight linear increase in surface pressure (2–3 mN/m). In contrast, isotherms of naturally occurring bovine brain GalCer are highly condensed (Ali et al., 1991, and references therein). The ΔV–A behavior for NFA-GalCer is shown in Figure 1B (curve a). At the onset of liquid-expanded behavior, ΔV is about 190 mV and rises continuously with film compression. Upon reaching 54 Å^2/molecule, the area corresponding to the onset of a two-dimensional phase transition, the slope of the ΔV–A isotherm also increases suddenly. Then, ΔV rises steeply until collapse begins at about 570 mV. Further compression reveals a decrease in the slope of the ΔV–A plot.

To determine the relative contribution of various GalCer species to NFA-GalCer's surface behavior, we compared the π–A behavior of several GalCer species. Of particular interest were GalCer species containing either long saturated or monounsaturated acyl chains because these species dominate NFA-GalCer's acyl composition [e.g., Johnson and Brown (1992) and references therein]. Initially, we determined the force–area behavior of N-24:0-GalSph. As illustrated in Figure 1A (curve b), the isotherm shows condensed behavior with no indication of the two-dimensional phase transition seen in NFA-GalCer. Also, π remains very low (< 1 mN/m) until the area reaches about 45 Å^2/molecule, at which point ΔV is about 400 mV. With continuous compression, the surface pressure rises steeply until the film begins to collapse near 60 mN/m. At collapse, ΔV reaches about 470 mV.

For comparison, we determined the force–area isotherms of GalCer bearing either stearoyl or palmitoyl acyl residues. These species were of interest because earlier DSC studies indicated that similar high-enthalpy, crystal to liquid crystal transition temperatures are observed for GalCer derivatives bearing palmitoyl, stearoyl, and lignoceroyl acyl chains (Ruocco et al., 1983; Curatolo & Jungalwala, 1985; Reed & Shipley, 1987; 1989). Panels A and B of Figure 1 show the π–A and ΔV–A isotherms, respectively, for N-18:0 GalSph (curve c) and for N-16:0 GalSph (curve d). It is clear that the range of ΔV and the slopes of the ΔV–A plots are similar to those of N-24:0-GalSph (curve b) and that these GalCer derivatives display condensed behavior with characteristic low compressibilities Table I (Table II). However, there are subtle features that distinguish the isotherms of each GalCer species. For instance, surface pressures above 1 mN/m are not detected until the area reaches 48 Å^2/molecule for N-18:0-GalSph and 53 Å^2/molecule for N-16:0-GalSph. Interestingly, N-18:0-GalSph's apparent collapse pressure and molecular area are similar to those of N-24:0-GalSph, while somewhat lower apparent collapse pressures and larger collapse areas are observed for N-16:0-GalSph (see Table I).

In any case, these results suggest that GalCer species other than those containing long, saturated acyl chains account for much of the π–A behavior observed in NFA-GalCer, i.e., the two-dimensional phase transition. The most likely candidates, based on NFA-GalCer's fatty acyl composition, would be GalCer species containing long acyl chains with single *cis* double bonds. Indeed, the major mono-unsaturated species in NFA-GalCer, N-24:1$^{\Delta 15}$-GalSph, displays liquid-expanded behavior at molecular areas between 82 and 65 Å^2/molecule (Figure 2A, curve a). Further compression results in a broad two-dimensional phase transition that commences near 65 Å^2/molecule at 10 mN/m. Over the next 25 Å^2/molecule,

Table I: Physical Parameters Derived from the Surface Pressure–Area (π–A) Isotherms (24 °C)

lipid species	π_t[d]	a_t[a]	ω_0	f_1	$\mu_\perp$	ΔV_0
N-24:0-GalSph	59.2	38.5	37.6	2.38	462	3.1
N-18:0-GalSph	60.5	39.6	36.6	1.85	611	−100.0
N-16:0-GalSph	55.8	44.4	40.6	1.81	486	10.0
N-10:0-GalSph	45.7	45.2	34.6	1.22	341	0.3
N-24:1$^{\Delta 15}$-GalSph	10.2[c] (46.7)[d]	65.4[c] (38.3)[d]	39.5	1.24	275 (1094)[d]	40.5 (−441)[d]
N-22:1$^{\Delta 13}$-GalSph	34.9[c] (46.0)[d]	49.9[c] (41.4)[d]	33.7	1.23	308 (506)[d]	26.0 (−122)[d]
N-20:1$^{\Delta 11}$-GalSph[b]	47.3	50.5	40.5	1.26	347	8.3
N-18:1$^{\Delta 9}$-GalSph[b]	47.9	51.5	42.0	1.25	365	1.0
N-20:2$^{\Delta 11,14}$-GalSph[b]	46.1	55.2	42.5	1.21	323	36.8
N-18:2$^{\Delta 9,12}$-GalSph	46.4	49.7	42.5	1.28	290	34.3
NFA-GalCer	8.9[c] (49.7)[d]	53.8[c] (39.3)[d]	29.8	1.19	497 (895)[d]	−63.0 (−309)[d]
bovine brain GalCer[b]	50.6	40.4	39.1	3.02	255	88

[a] π_t is the collapse pressure (mN/m), and A_t is the collapse area (Å^2/molecule). Other parameters were calculated as described under Materials and Methods. [b] Similar to values reported previously (Ali et al., 1991). Here they are the mean of 2–5 different isotherms rather than a single representative isotherm. [c] Values for the two-dimensional phase transition, in which case π_t is the onset pressure (mN/m) and A_t is the molecular area (Å^2/molecule). [d] Values derived from the condensed portion of the isotherms.

Table II: Lipid Compressibilities (k)[a]

	5.0 mN/m		15 mN/m		30 mN/m	
lipid	area (Å^2)	k (×10^{-3} m/mN)	area (Å^2)	k (×10^{-3} m/mN)	area (Å^2)	k (×10^{-3} m/mN)
N-24:0-GalSph	43.6	5.79	41.8	3.04	40.3	2.00
N-18:0-GalSph	46.2	6.17	44.4	4.08	42.2	2.84
N-16:0-GalSph	51.8	6.78	49.3	4.01	46.9	2.97
N-10:0-GalSph	67.3	23.5	58.9	13.3	50.5	7.85
N-24:1$^{\Delta 15}$-GalSph	70.1	20.3	39.2	6.87	37.3	2.67
N-22:1$^{\Delta 13}$-GalSph	68.3	18.4	59.6	11.4	51.4	9.2
N-20:1$^{\Delta 11}$-GalSph	70.4	18.2	61.7	10.1	54.9	6.44
N-18:1$^{\Delta 9}$-GalSph	71.7	19.5	62.5	10.4	55.7	5.97
N-20:2$^{\Delta 11,14}$-GalSph	80.0	20.5	68.9	10.4	60.5	7.18
N-18:2$^{\Delta 9,12}$-GalSph	68.8	20.1	59.7	10.3	53.3	5.94
NFA-GalCer	61.4	40.7[b]	42.5	4.68	40.5	2.33
bovine brain GalCer	43.3	3.0	42.3	1.92	41.3	1.41

[a] Compressibilities were calculated as described under Materials and Methods. [b] This high compressibility value is indicative of a low-pressure transition which becomes more clearly evident at higher temperatures (unpublished observation).

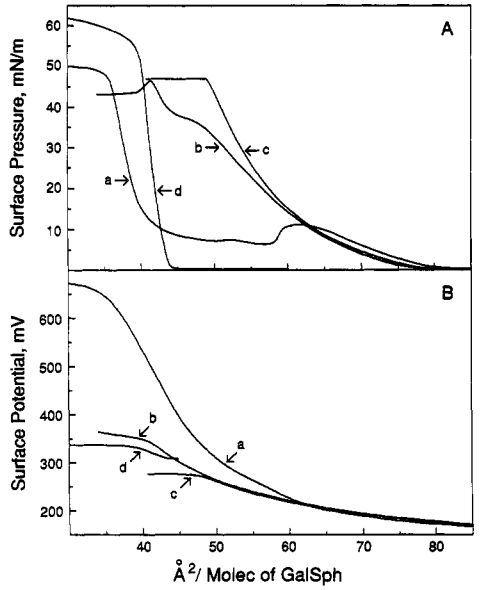

FIGURE 2: (A) Surface pressure vs molecular area (π–A) and (B) surface potential vs molecular area (ΔV–A) isotherms. Data were collected at 24°C as described under Materials and Methods for (a) *N*-24:1$^{\Delta 15}$-GalSph, (b) *N*-22:1$^{\Delta 13}$-GalSph, (c) *N*-18:2$^{\Delta 9,12}$-GalSph, and (d) bovine brain GalCer.

a somewhat metastable transformation occurs until a condensed state is achieved. Apparent film collapse occurs near 49 mN/m. Shortening the acyl chain by two carbons (*N*-22:1$^{\Delta 13}$-GalSph; curve b) elevates the surface pressure and diminishes the molecular area at which the two-dimensional phase transition occurs and slightly lowers the apparent collapse pressure (47.5 mN/m). Further decreases in the length of the mono-unsaturated acyl chain (e.g., *N*-20:1$^{\Delta 11}$-GalSph or *N*-18:1$^{\Delta 9}$-GalSph) produce films that display only liquid-expanded behavior at 24°C and apparent collapse at 47.2 and 46.9 mN/m, respectively (Ali et al., 1991). Compressibilities characteristic of liquid-expanded and liquid-condensed phases are obtained at appropriate surface pressures (Table II).

Figure 2B shows the ΔV–A behavior of the GalCer species with mono-unsaturated acyl chains (curves a and b). At areas between 75 and 80 Å^2/molecule, ΔV values are all about 190 mV. Upon compression of this GalCer species, the ΔV–A behavior is very similar to that observed for other liquid-expanded GalCer species (Ali et al., 1991) until the onset of the two-dimensional phase transitions. Thereafter, the slopes increase noticeably. Then, when the apparent collapse pressure is reached, ΔV levels off. Such behavior has also been observed for other lipids including phospholipids like DPPC [e.g., Cadenhead et al. (1967) and Vogel and Möbius (1988)].

Liquid-expanded films are also obtained if, rather than introducing unsaturation, one shortens sufficiently the length of the saturated acyl chain in GalCer. Figure 1A (curve e) shows the force–area behavior of the GalCer derivative containing decanoyl (10:0) acyl chains. At 1 mN/m, the molecular area is near 80 Å^2/molecule and ΔV is about 180 mV. Upon further GalCer compression, the surface pressure rises continuously until apparent collapse occurs at 45.8 mN/m (44.9 Å^2/molecule) and ΔV has reached about 300 mV. As shown in Table I, this molecular area is intermediate between those measured for GalCer derivatives with long saturated acyl chains (e.g., *N*-24:0-GalSph and *N*-18:0-GalSph) and

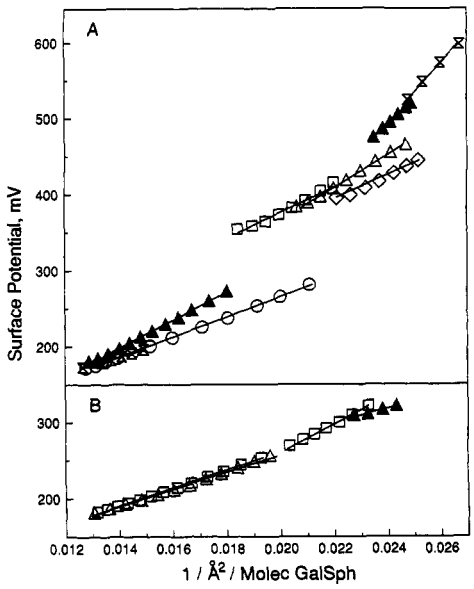

FIGURE 3: Surface potential vs inverse molecular area. Data were collected as described under Materials and Methods. Panel A includes the lipids whose isotherms appear in Figure 1: (◇) *N*-24:0-GalSph; (△) *N*-18:0-GalSph; (□) *N*-16:0-GalSph; (○) *N*-10:0-GalSph; (⧖) *N*-24:1$^{\Delta 15}$-GalSph; (▲) *N*-NFA-GalCer. Panel B includes the lipids whose isotherms appear in Figure 2: (□) *N*-22:1$^{\Delta 13}$-GalSph; (△) *N*-18:2$^{\Delta 9,12}$-GalSph; (▲) bovine brain GalCer.

those that we and others previously reported for liquid-expanded GalCer derivatives with mono-unsaturated acyl chains (e.g., *N*-18:1$^{\Delta 9}$-GalSph and *N*-20:1$^{\Delta 11}$-GalSph) (Johnston & Chapman, 1988; Ali et al., 1991). Interestingly, the range of *N*-10:0 GalSph's ΔV values and the slopes of the ΔV–A plots are quite similar to those previously noted for liquid-expanded GalCer derivatives with unsaturated acyl chains (Ali et al., 1991).

Not surprisingly, liquid-expanded behavior also occurs if two *cis* double bonds are present in GalCer's acyl chain (e.g., *N*-18:2$\Delta^{9,12}$; Figure 2A, curve c). Similar findings have been reported for the π–A isotherms of *N*-20:2$^{\Delta 11,14}$-GalSph (Ali et al., 1991) and monogalactosyl diglyceride (MGDG) containing linolenoyl acyl chains (Sen et al., 1981).

Other characteristics of these GalCer derivatives are revealed by analyzing the isotherms with an equation of state for lipid monolayers (Smaby & Brockman, 1991b). Although this equation of state has been shown to be valid for several different lipids displaying liquid-expanded behavior, its applicability to condensed films is less clear (see Materials and Methods). Table I shows the resulting values for the collapse areas (A_t) and the dehydrated molecular areas (ω_0) for each GalCer derivative determined as described under Materials and Methods. In general, the values are consistent with the physico-chemical behavior predicted for different fatty acyl structures.

Previously we reported that plots of ΔV versus $1/A$ are linear for three different liquid-expanded GalCer derivatives containing unsaturated acyl chains (Ali et al., 1991). In fact, the linearity of ΔV versus $1/A$ plots extends to a variety of liquid-expanded, glycerol-based lipids as well as to long-chain acyl derivatives (Smaby & Brockman, 1990). What is not clear from these earlier studies is whether such plots yield linear behavior for condensed phase lipids. Figure 3 shows that all the condensed GalCer derivatives in this study do yield linear ΔV versus $1/A$ behavior and validates this approach for determining the $\mu_\perp$ values shown in Table I. Also, the GalCer derivatives that display two-dimensional phase transitions (*N*-24:1Δ^{15}-GalSph, NFA-GalCer) have two distinct linear regions which correspond to their liquid-expanded and -condensed phases. Resulting $\mu_\perp$ values are shown in Table I.

DISCUSSION

Although no systematic investigation of the surface behavior of individual GalCer molecular species has been reported previously, the π–A behavior of a few homogeneously *N*-acylated GalSpd derivatives has been studied. In general, our π–A results for *N*-16:0-GalSph agree well with the π–A isotherm of *N*-16:0-Gal dihydroSph reported by Oldani et al. (1975) under similar, but not identical, conditions. Not surprisingly, greater differences are observed between our isotherms for *N*-18:0-GalSph and earlier data which were measured at 37 °C over a subphase of pure water (Johnston & Chapman, 1988). The major differences occurred in the low-pressure region of the condensed isotherms. In any case, the condensed behavior of *N*-18:0-GalSph is clearly different from the π–A behavior of monogalactosyl diglyceride (MGDG) bearing stearoyl acyl chains. This MGDG derivative displays a liquid-expanded to liquid-condensed (LE–LC) transition at 20 °C [e.g., Tomoaia-Cotisel et al. (1989)]. Such findings indicate that, at room temperature, the intermolecular interactions in surface films of *N*-18:0-GalSph are stronger than those in distearoyl MGDG monolayers. A likely explanation for this behavior is the following: In 18:0-GalSph, the interfacial amide linkages provide extra intermolecular attractive forces in the form of hydrogen bonds in addition to the van der Waal's interactions that occur between the hydrocarbon chains. The existence of this hydrogen bonding capability for sphingolipids was revealed many years ago [e.g., Bunow and Levin (1980)]. More recently, the importance of amide linkages in stabilizing lipid assemblies has also been reported for artificial phospholipids (Sunamoto et al., 1990a,b). This stabilization is also thought to occur because of interfacial hydrogen-bonding involving both direct interactions between neighboring lipids as well as intermolecular hydration reactions through polarized water molecules.

The condensed behavior (Figure 1A) and very low compressibilities (Table II) of GalCer species containing lignocerate, stearate, or palmitate acyl chains are consistent with their known thermotropic properties. DSC measurements of hydrated dispersions have revealed high (~82°C) crystal to liquid crystalline phase-transition temperatures that change little regardless of whether the acyl chain is palmitate, stearate, or lignocerate (Ruocco et al., 1983; Curatolo & Jungalwala, 1985; Reed & Shipley, 1987, 1989). In excess water, these lipids form bilayers and the derivatives possessing asymmetric hydrocarbon chains (e.g., *N*-24:0-GalSph) partially interdigitate to optimize their van der Waal's attractive interactions in the gel and crystalline phases. In monolayers, chain–chain interdigitation is energetically unfavorable. This property of monolayers permits intermolecular interactions to be studied in the absence of interdigitation and, by comparison to bilayers, provides insight into the role which acyl chain interdigitation plays in modulating GalCer's behavior in membranes. Indeed, our π–A isotherms do reveal interesting features not apparent in the DSC/X-ray studies of GalCer bilayers. At a given temperature and surface pressure, the molecular area for these GalCer species decreases with increasing fatty acyl chain length. This is clearly evident from the "lift-off" and apparent collapse areas and most likely reflects the rise in van der Waal's attractive forces that accompanies increasing acyl chain length (Salem, 1962). To achieve the close intermolecular approach

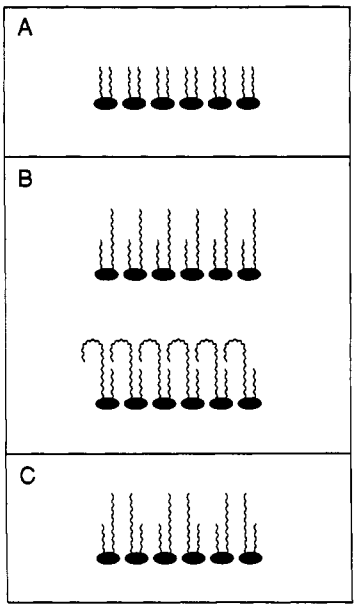

FIGURE 4: Possible monolayer configurations of GalCer derivatives. For simplicity, the molecular tilt is not depicted although it is known to occur in condensed phases of phospholipids [e.g., Helm et al. (1991)]. Panel A shows an arrangement for *N*-16:0-GalSph. On the basis of X-ray studies [e.g., Ruocco et al. (1981) and Pascher et al. (1992)], the hydrocarbon chains in *N*-16:0-GalSph would be effectively symmetric in length. Panel B shows energetically unfavorable arrangements for *N*-24:0-GalSph. Because the acyl chain is much longer than the sphingolipid base, a large intramolecular asymmetry exists with respect to hydrocarbon chain length. Panel C shows an energetically favorable average orientation for condensed *N*-24:0-GalSph monolayers. This arrangment would maximize intermolecular van der Waal's interactions.

needed to optimize the van der Waal's attractive interactions among GalCer molecules with two hydrocarbon chains of highly asymmetric length, molecules like *N*-24:0-GalSph probably assume average orientations that maximize their intermolecular chain–chain alignments in the condensed monolayer state. Figure 4C shows such an arrangement. If correct, considerable long-range order might exist, not only because of the van der Waal's interactions but also because of the intermolecular hydrogen bonding that occurs in condensed GalCer surfaces [e.g., Bunow and Levin (1980) and Pink et al. (1988)].

The fact that the GalCer species with saturated acyl chains can achieve such low molecular areas prior to collapse also suggests that the galactose headgroup extends into the aqueous subphase rather than lying parallel with the argon–buffered saline interfacial plane. This latter "shovel" conformation has been reported for crystalline GalCer, but requires 51.9 Å^2/molecule as a minimal interfacial area [e.g., Pascher et al. (1992)]. Thus, on the basis of interfacial geometry, GalCer cannot assume the "shovel" conformation even in highly condensed crystalline-like films. The intra- and intermolecular hydrogen bonding system responsible for the shovel conformation in crystalline GalCer must be significantly relaxed under fully hydrated conditions. This also appears to be the case for GalCer bilayer assemblies (Bunow & Levin, 1980; Skarjune & Oldfield, 1982).

From our ΔV–A data of GalCer species containing long, saturated acyl chains, it is clear that ΔV increases almost linearly over the entire range of condensed π–A behavior for each GalCer species. With the exception of one other study (Oldani et al., 1975), the ΔV–A behavior of chain-pure glycosphingolipids has not been reported previously. Oldani et al. (1975) examined the ΔV–A behavior of *N*-16:0-Gal dihydroSph and reported values significantly higher (~100 mV) than ours. The results are puzzling because the π–A data for these two 16:0 derivatives matched very well, and if anything, we expected *N*-16:0-GalSph's ΔV values to be higher than *N*-Gal-dihydroSph's because hydrogenation of the 4,5-*trans* double bond in the sphingosine base of sphingomyelin reportedly lowers ΔV (Shah & Schulman, 1967).

In any case, the ΔV values for GalCer species containing long saturated acyl chains are greater (~100 mV) than those of bovine brain GalCer, but are smaller (~75 mV) than those of NFA-GalCer when compared at molecular areas corresponding to 30–35 mN/m, surface pressures similar to those in biological membranes. Indeed, we have recently observed that the ΔV values of a GalCer fraction containing only 2-hydroxy acyl chains (HFA-GalCer) are smaller than those of naturally occurring bovine brain GalCer at molecular areas corresponding to 30 mN/m (unpublished observation). Thus, a major role of HFA-GalCer may be that of modulating the potential of membranes like myelin.

In any event, it is clear from our earlier studies that certain structural alterations to GalCer molecules, such as the introduction of unsaturation into acyl moieties, can prevent strong cohesive interactions from occurring (Ali et al., 1991). For this reason, we were interested in whether a short saturated acyl chain could fulfill a similar role in GalCer. Although we do find differences in the isotherms of *N*-10:0-GalSph and GalCer species containing either oleoyl, eicosenoyl, or eicosadienoyl acyl moieties (Ali et al., 1991) (e.g., apparent collapse areas, lift-off areas, compressibilities), they all form stable liquid-expanded films at 24 °C. Moreover, their average interfacial molecular orientations, as measured by the ΔV–A behavior, are almost identical. Previously, other investigators have noted that PCs and PEs bearing two short, saturated acyl chains form liquid-expanded films at 22 °C (Phillips & Chapman, 1968). We have also observed similar behavior in 1-stearoyl-2-capryl PC films (unpublished observation).

From the present study, it appears that, in the physiological temperature range, introducing a single *cis* double bond into a long saturated acyl chain like lignocerate has much greater impact on GalCer's intermolecular interactions than reducing the acyl chain length by six or eight carbons. Whereas *N*-16:0-GalSph displays only condensed behavior at 24°C, *N*-24:1$^{\Delta 15}$-GalSph displays liquid-expanded behavior at low surface pressures and undergoes a distinct two-dimensional phase transition into a condensed film with increasing surface pressure. At surface pressures in the transition region (7–10 mN/m), the compressibilities reach values between 55 and 60×10^{-3} m/mN but then, upon further compression, sharply drop to values characteristic of condensed monolayer phases (Table II). This finding is reasonable for a monolayer phase transition because the boundary defects in the coexistence region of liquid-expanded and -condensed phases causes a sudden "spike" in compressibility [e.g., Tomoaia-Cotisel et al. (1989) and Mouritsen et al. (1989)]. Finding two-dimensional phase transitions in GalCer species like *N*-24:1$^{\Delta 15}$-GalSph and *N*-22:1$^{\Delta 13}$-GalSph was anticipated because we observed similar transitions below 15°C for *N*-20:1$^{\Delta 11}$-GalSph and for *N*-18:1$^{\Delta 9}$-GalSph (unpublished observations). Also, a two-dimensional phase transition had been reported in the π–A isotherm of NFA-GalCer at 37 °C (Johnston & Chapman, 1988) but not at 22°C (Oldani et al., 1975).

The π–A behavior of *N*-24:1$^{\Delta 15}$-GalSph, which accounts for 30% of NFA-GalCer's molecular composition [e.g., Johnson and Brown (1992)], is particularly intriguing because of the apparent metastability which its two-dimensional phase

transition displays. We are currently investigating this behavior in more detail. Also, *N*-24:1$^{\Delta 15}$-GalSph's π–*A* behavior clearly indicates that this GalCer species plays a dominant role in governing NFA-GalCer's interfacial properties. Our isotherms for NFA-GalCer displayed behavior very similar to those of *N*-24:1$^{\Delta 15}$-GalSph except that NFA-GalCer's two-dimensional phase transition occurred at smaller molecular areas and its films reached higher pressures prior to collapse. These differences are reasonable considering the high content of *N*-24:0-GalSph (~30 mol %) also known to occur in NFA-GalCer [e.g., Johnson and Brown (1992)]. The π–*A* behavior which we observed for NFA-GalCer was markedly different from the condensed behavior reported earlier (Oldani et al., 1975). Because our π–*A* data for *N*-16:0-GalSph agrees so well with their data for *N*-16:0-GaldihydroSph, we can only speculate that sample differences, such as drastically lower *N*-24:1$^{\Delta 15}$-GalSph content, are responsible rather than experimental differences. NFA-GalCer's two-dimensional phase transition has also been observed by Johnston and Chapman (1988). However, in contrast to our highly reproducible isotherms, their data showed variations of up to 8 Å^2/molecule in the onset of NFA-GalCer's two-dimensional phase transition [e.g., Johnston and Chapman (1988); Figure 1 vs 2). We believe that this is due to experimental differences (e.g., subphase composition, temperature, compression rate, π detection method).

Not only the presence but also the location of the *cis* double bond in GalCer's acyl chain has dramatic effects on the molecule's interfacial behavior. As *N*-24:1$^{\Delta 15}$-GalSph's acyl chain is shortened successively by two carbons while keeping the *cis* double bond at the ω^9 position, the isotherms respond in a predictable manner. For instance, *N*-22:1$^{\Delta 13}$-GalSph requires higher pressures than *N*-24:1$^{\Delta 15}$-GalSph to induce the onset of the two dimensional phase transition. Additional shortening of the acyl chain while the *cis* double bond is kept at the ω^9 position (e.g., *N*-20:1$^{\Delta 11}$-GalSph and *N*-18:1$^{\Delta 9}$-GalSph) completely eliminates the two-dimensional phase transition from the 24 °C force–area curves (Ali et al., 1991).

Aside from regulation of the two-dimensional phase state of GalCer, another important effect of *cis* double bond position in GalCer's acyl chain relates to the surface potential. It is well known that the presence of a *cis* double bond disorders hydrocarbon chain packing and causes a drop in the molecular dipole moment and the observed surface potential [e.g., Harkins and Fischer (1933) and Hühnerfuss (1989)]. Because the number of CH_2 groups contributes little to the molecular dipole moment (Vogel & Möbius, 1988) and the molecular conformation and orientation of functional groups at the lipid–water interface remains relatively constant [e.g., Smaby and Brockman (1990)], the drop in $\mu_\perp$ can be attributed, in large part, to an increase in motional freedom of the hydrocarbon's terminal methyl group. The dipole moment of the terminal methyl group within a close-packed monolayer is +0.35 D (Vogel & Möbius, 1988). What is not clear is the effect of double bond position on the molecular dipole moment. As shown in Table I, all of the GalCer derivatives displaying liquid-expanded isotherms have similar ΔV–*A* behavior regardless of the presence and position of the acyl chain double bond. However, the position of the *cis* double bond has a major impact on the ΔV values (Figures 1B and 2B) and the dipole moments in the condensed phases (Table I). For instance, *N*-24:1$^{\Delta 15}$-GalSph reaches values of over 600 mV at molecular areas corresponding to 40 mN/m. The resulting surface dipole moment is 1.2-fold higher than that observed for condensed NFA-GalCer, but over 4-fold higher than that of bovine brain GalCer. In contrast, *N*-22:1$^{\Delta 13}$-GalSph only reaches about 340 mV with a resulting dipole moment about half that of *N*-24:1$^{\Delta 15}$-GalSph. Because changing the length of saturated acyl chains in condensed GalCer films has only modest effects on the ΔV–*A* behavior, these observations indicate that the position of the *cis* double bond relative to the hydrocarbon–argon interface contributes substantially to the molecular dipole and the observed ΔV (Table I). Indeed, in the case of *N*-24:1$^{\Delta 15}$-GalSph, the *cis* double bond would be positioned very near the hydrocarbon–argon interface. Shortening of the acyl chain while maintaining the *cis* double bond at the ω^9 position with respect to the acyl chain's terminal methyl group would effectively place the double bond deeper and deeper into the hydrocarbon monolayer matrix.

Implications. From this study we conclude that changing GalCer's acyl chain length has relatively modest effects on GalCer's interfacial interactions when the acyl chain is long and saturated. However, introducing a single *cis* double bond into GalCer's acyl chain makes the lipid's interfacial interactions much more responsive to changes in acyl chain length. An important physiological consequence may be better accommodation of lipids like cholesterol in lamellar assemblies of GalCer. In nature, high cholesterol concentrations are often found in membranes containing relatively high amounts of GalCer and other simple sphingolipids. The interaction of cholesterol with various GalCer derivatives is currently under investigation.

ACKNOWLEDGMENT

We thank Howard Brockman for the use of the Langmuir film balance and for critically evaluating the manuscript. We also thank C. Perleberg and J. Ruble for typing services.

REFERENCES

Ali, S., Brockman, H. L., & Brown, R. E. (1991) *Biochemistry 30*, 11198-11205.
Ali, S., Brockman, H. L., & Brown, R. E. (1992a) *Biophys. J. 61*, A375.
Ali, S., Brockman, H. L., & Brown, R. E. (1992b) *FASEB J. 6*, A375.
Alvarez, J. G., Touchstone, J. C., Storey, B. T., & Grob, R. L. (1989) *J. Liq. Chromatogr. 12*, 3115–3120.
Bhat, S., Spitalnik, S. L., Gonzalez-Scarano, F., & Silberberg, D. H. (1991) *Proc. Natl. Acad. Sci. U.S.A. 88*, 7131–7134.
Brockman, H. L., Jones, C. M., Schwebke, C. J., Smaby, J. M., & Jarvis, D. E. (1980) *J. Colloid Interface Sci. 78*, 502–512.
Brockman, H. L., Smaby, J. M., & Jarvis, D. E. (1984) *J. Phys. E: Sci. Instrum. 17*, 351–353.
Bunow, M. R. (1979) *Biochim. Biophys. Acta 574*, 542–546.
Bunow, M. R., & Levin, I. W. (1980) *Biophys. J. 32*, 1007–1021.
Cadenhead, D. A., Demchak, R. J., & Phillips, M. C. (1967) *Kolloid Z. Z. Polym. 220*, 59–64.
Curatolo, W. (1982) *Biochemistry 21*, 1761–1764.
Curatolo, W. (1987) *Biochim. Biophys. Acta 906*, 111–136.
Curatolo, W., & Jungalwala, F. B. (1985) *Biochemistry 24*, 6608–6613.
Gaines, G. L., Jr. (1966) *Insoluble Monolayers at Liquid/Gas Interfaces*, pp 73–89, Wiley-Interscience, New York.
Gardam, M., & Silvius, J. R. (1989) *Biochim. Biophys. Acta 980*, 319–325.
Hakomori, S. (1990) *J. Biol. Chem. 265*, 18713–18716.
Hannun, Y. A., & Bell, R. M. (1989) *Science 243*, 500–507.
Harkins, W. D., & Fischer, E. K. (1933) *J. Chem. Phys. 1*, 852–862.
Hühnerfuss, H. (1989) *J. Colloid Interface Sci. 128*, 237–244.
Harouse, J. M., Bhat, S., Spitalnik, S., Spitalnik, S. L., Laughlin, M., Stefano, K., Silberberg, D. H., & Gonzalez-Scarano, F. (1991) *Science 253*, 320–323.

Helm, C. A., Tippmann-Krayer, P., Möhwald, H., & Kjaer, K. (1991) *Biophys. J. 60*, 1457–1476.
Jackson, M., Johnston, D. S., & Chapman, D. (1988) *Biochim. Biophys. Acta 944*, 497–506.
Johnson, S. B., & Brown, R. E. (1992) *J. Chromatogr. 605*, 281–286.
Johnston, D. S., & Chapman, D. (1988) *Biochim. Biophys. Acta 937*, 10-22.
Karlsson, K.-A. (1989) *Annu. Rev. Biochem. 58*, 309–350.
Kishimoto, Y., Moser, H. W., & Suzuki, K. (1985) in *Handbook of Neurochemistry* (Lajtha, A., Ed.) Vol. 10, pp 125–151, Plenum Press, New York.
Kubo, H., & Hoshi, M. (1985) *J. Lipid Res. 26*, 638–641.
Ledeen, R. W. (1984) *J. Neurosci. Res. 12*, 147–159.
Lee, D. C., Miller, I. R., & Chapman, D. (1986) *Biochim. Biophys. Acta 859*, 266–270.
Middleton, S. R., & Pethica, B. A. (1981) *Faraday Symp. Chem. Soc. 16*, 109–123.
Mouritsen, O. G., Ipsen, J. H., & Zuckermann, M. J. (1989) *J. Colloid Interface Sci. 129*, 32–40.
Oldani, D., Hauser, H., Nichols, B. W., & Phillips, M. C. (1975) *Biochim. Biophys. Acta 382*, 1–9.
Pascher, I., Lundmark, M., Nyholm, P.-G., & Sundell, S. (1992) *Biochim. Biophys. Acta 1113*, 339–373.
Phillips, M. C., & Chapman, D. (1968) *Biochim. Biophys. Acta 163*, 310-313.
Pink, D. A., MacDonald, A. L., & Quinn, B. (1988) *Chem. Phys. Lipids 47*, 83–95.
Radin, N. S. (1974) *Lipids 9*, 358–360.
Reed, R. A., & Shipley, G. G. (1987) *Biochim. Biophys. Acta 896*, 153–164.
Reed, R. A., & Shipley, G. G. (1989) *Biophys. J. 55*, 281–292.
Ruocco, M. J., Atkinson, D. M., Small, D. M., Skarjune, R. P., Oldfield, E., & Shipley, G. G. (1981) *Biochemistry 20*, 5957–5966.
Ruocco, M. J., Shipley, G. G., & Oldfield, E. (1983) *Biophys. J. 43*, 91–101.
Salem, L. (1962) *J. Chem. Phys. 37*, 2100–2113.
Sen, A., Williams, W. P., & Quinn, P. J. (1981) *Biochim. Biophys. Acta 663*, 380–389.
Shah, D. O., & Schulman, J. H. (1967) *J. Lipid Res. 8*, 215–233.
Skarjune, R., & Oldfield, E. (1982) *Biochemistry 21*, 3154–3160.
Smaby, J. M., & Brockman, H. L. (1985) *Biophys. J. 48*, 701–708.
Smaby, J. M., & Brockman, H. L. (1990) *Biophys. J. 58*, 195–204.
Smaby, J. M., & Brockman, H. L. (1991a) *Chem. Phys. Lipids 58*, 249–252.
Smaby, J. M., & Brockman, H. L. (1991b) *Langmuir 7*, 1031–1034.
Sunamoto, J., Goto, M., Iwamoto, K., Kondo, H., & Sato, T. (1990a) *Biochim. Biophys. Acta 1024*, 209–219.
Sunamoto, J., Nagai, K., Goto, M., & Lindman, B. (1990b) *Biochim. Biophys. Acta 1024*, 220–226.
Suzuki, K., & Suzuki, Y. (1989) in *The Metabolic Basis of Inherited Disease II* (Scriver, C. M., Beaudet, A. L., Sly, W. S., & Valle, D., Eds.) 6th ed., pp 1699–1720, McGraw-Hill, San Francisco.
Thompson, T. E., & Tillack, T. W. (1985) *Annu. Rev. Biophys. Biophys. Chem. 14*, 361–386.
Tomoaia-Cotisel, M., Zsako, J., Chifu, E., & Quinn, P. J. (1989) *Chem. Phys. Lipids 50*, 127–133.
Vogel, V., & Möbius, D. (1988) *J. Colloid Interface Sci. 126*, 408–420.
Yokoyama, S., & Kézdy, F. J. (1991) *J. Biol. Chem. 266*, 4303–4308.